LA-UR-96-4583

...d for public release;
...ion is unlimited.

Title: TREATING ELECTRON TRANSPORT IN MCNP™

Author(s): H. Grady Hughes

Submitted to: Proceedings of the training course on the use of MCNP in Radiation Protection and Dosimetry held in Bologna - Italy, May 13 - 16, 1996

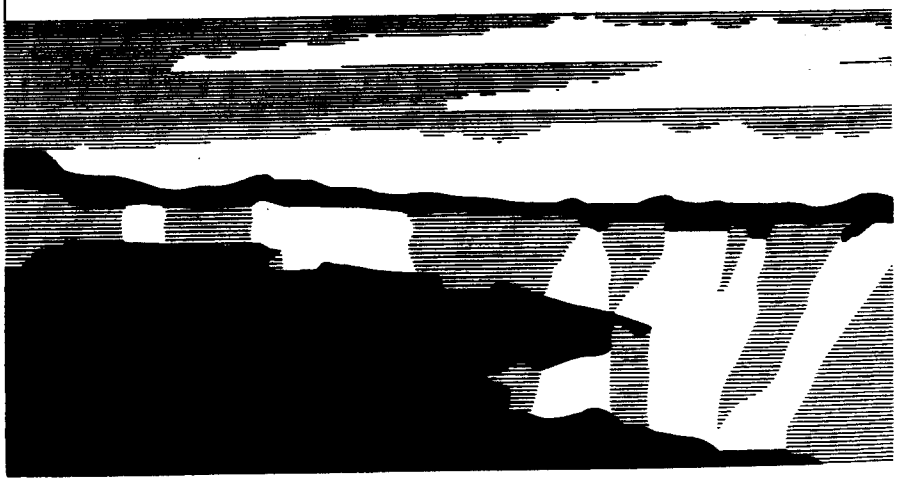

Los Alamos
NATIONAL LABORATORY

Treating Electron Transport in MCNP™

H. Grady Hughes

1. Introduction

The transport of electrons and other charged particles is fundamentally different from that of neutrons and photons. The interaction of neutral particles is characterized by relatively infrequent isolated collisions, with simple free flight between collisions. By contrast, the transport of electrons is dominated by the long-range Coulomb force, resulting in large numbers of small interactions. For example, a neutron in aluminum slowing down from 0.5 MeV to 0.0625 MeV will have about 30 collisions, while a photon in the same circumstances will experience fewer than ten. An electron accomplishing the same energy loss will undergo about 10^5 individual interactions. This great increase in computational complexity makes a single-collision Monte Carlo approach to electron transport infeasible for many situations of practical interest.

Considerable theoretical work has been done to develop a variety of analytic and semi-analytic multiple-scattering theories for the transport of charged particles. These theories attempt to use the fundamental cross sections and the statistical nature of the transport process to predict probability distributions for significant quantities, such as energy loss and angular deflection. The most important of these theories for the algorithms in MCNP* are the Goudsmit-Saunderson[1] theory for angular deflections, the Landau[2] theory of energy-loss fluctuations, and the Blunck-Leisegang[3] enhancements of the Landau theory. These theories rely on a variety of approximations that restrict their applicability, so that they cannot solve the entire transport problem. In particular, it is assumed that the energy loss is small compared to the kinetic energy of the electron.

In order to follow an electron through a significant energy loss, it is necessary to break the electron's path into many steps. These steps are chosen to be long enough to encompass many collisions (so that multiple-scattering theories are valid) but short enough that the mean energy loss in any one step is small (so that the approximations necessary for the multiple-scattering theories are satisfied). The energy loss and angular deflection of the electron during each of the steps can then be sampled from probability distributions based on the appropriate multiple-scattering theories. This subsumption of the effects of many individual collisions into single steps that are sampled probabilistically constitutes the "condensed history" Monte Carlo method.

The most influential reference for the condensed history method is the 1963 paper by Martin J. Berger.[4] Based on the techniques described in that work, Berger and Stephen M. Seltzer developed the ETRAN series of electron/photon transport codes.[5] These codes have been main-

* MCNP is a trademark of the Regents of the University of California, Los Alamos National Laboratory.

tained and enhanced for many years at the National Bureau of Standards (now the National Institute of Standards and Technology). The ETRAN codes are also the basis for the Integrated TIGER Series,[6] a system of general-purpose, application-oriented electron/photon transport codes developed and maintained by John A. Halbleib and his collaborators at Sandia National Laboratories in Albuquerque, New Mexico. The electron physics in MCNP is similar to that of the Integrated TIGER Series.

2. Electron Steps and Substeps

The condensed random walk for electrons can be considered in terms of a sequence of sets of values

$$(0, E_0, t_0, \vec{\mathbf{u}}_0, \vec{\mathbf{r}}_0), (s_1, E_1, t_1, \vec{\mathbf{u}}_1, \vec{\mathbf{r}}_1), (s_2, E_2, t_2, \vec{\mathbf{u}}_2, \vec{\mathbf{r}}_2), \ldots$$

where s_n, E_n, t_n, $\vec{\mathbf{u}}_n$ and $\vec{\mathbf{r}}_n$ are the total path length, energy, time, direction, and position of the electron at the end of n steps. On the average, the energy and path length are related by

$$E_{n-1} - E_n = -\int_{s_{n-1}}^{s_n} \frac{dE}{ds} ds \tag{1}$$

where $-dE/ds$ is the total stopping power in energy per unit length. This quantity depends on energy and on the material in which the electron is moving. ETRAN-based codes customarily choose the sequence of path lengths $\{s_n\}$ such that

$$\frac{E_n}{E_{n-1}} = k \tag{2}$$

for a constant k. The most commonly used value is $k = 2^{-1/8}$, which results in an average energy loss per step of 8.3%.

Electron steps with (energy-dependent) path lengths $s = s_n - s_{n-1}$ determined by Equations 1–2 are called *major steps* or *energy steps*. The condensed random walk for electrons is structured in terms of these energy steps. For example, all precalculated and tabulated data for electrons are stored on an energy grid whose consecutive energy values obey the ratio in Equation 2. In addition, the Landau and Blunck-Leisegang theories for energy straggling are applied once per energy step. For a single step, the angular scattering could also be calculated with satisfactory accuracy, since the Goudsmit-Saunderson theory is valid for arbitrary angular deflections. However, the representation of the electron's trajectory as the result of many small steps will be more accurate if the angular deflections are also required to be small. Therefore, the ETRAN codes and MCNP further

break the electron steps into smaller substeps. A major step of path length s is divided into m substeps, each of path length s/m. Angular deflections and the production of secondary particles are sampled at the level of these substeps. The integer m depends only on material (average atomic number Z). Appropriate values for m have been determined empirically, and range from $m = 2$ for $Z < 6$ to $m = 15$ for $Z > 91$.

In some circumstances, it may be desirable to increase the value of m for a given material. In particular, a very small material region may not accommodate enough substeps for an accurate simulation of the electron's trajectory. In such cases, the user can increase the value of m with the ESTEP option on the material card. The user can gain some insight into the selection of m by consulting Print Table 85 in the MCNP output. Among other information, this table presents a quantity called DRANGE as a function of energy. DRANGE is the size of an energy step in gm/cm^2. Therefore, DRANGE/m is the size of a substep in the same units, and if ρ is the material density in gm/cm^3, then the quantity $\mathrm{DRANGE}/(m\rho)$ is the length of a substep in cm. This quantity can be compared with the smallest dimension of a material region. A reasonable goal is that an electron should make at least ten substeps in any material of importance to the transport problem.

3. Condensed Random Walk

In the initiation phase of a transport calculation involving electrons, all relevant data are either precalculated or read from the electron data file and processed. These data include the electron energy grid, stopping powers, electron ranges, energy step lengths, substep lengths, and probability distributions for angular deflections and for the production of secondary particles. Although the energy grid and electron steps are selected according to Equations 1–2, energy straggling, the analog production of bremsstrahlung, and the intervention of geometric boundaries and the problem time cutoff will cause the electron's energy to depart from a simple sequence $\{E_n\}$ satisfying Equation 2. Therefore, the necessary parameters for sampling the random walk will be interpolated from the points on the energy grid.

At the beginning of each major step, the collisional energy loss rate is sampled. In the absence of energy straggling, this will be a simple average value based on the nonradiative stopping power described in the next section. In general, however, fluctuations in the energy loss rate will occur. The number of substeps m per energy step will have been preset, either from the empirically-determined default values, or by the user, based on geometric considerations. At most m substeps will be taken in the current major step, *i.e.* with the current value for the energy loss rate. The number of substeps may be reduced if the electron's energy falls below the boundary of the current major step, or if the electron reaches a geometric boundary. In these circumstances, or upon the completion of m substeps, a new major step is begun, and the energy loss rate is resampled.

Except for the energy loss and straggling calculation, the detailed simulation of the electron history takes place in the sampling of the substeps. The Goudsmit-Saunderson[1] theory is used to sample from the distribution of angular deflections, so that the direction of

the electron can change at the end of each substep. Based on the current energy loss rate and the substep length, the projected energy for the electron at the end of the substep is calculated. Finally, appropriate probability distributions are sampled for the production of secondary particles. These include electron-induced fluorescent X-rays, "knock-on" electrons (from electron-impact ionization), and bremsstrahlung photons.

Note that the length of the substep ultimately derives from the total stopping power used in Equation 1, but the projected energy loss for the substep is based on the nonradiative stopping power. The reason for this difference is that the sampling of bremsstrahlung photons is treated as an essentially analog process. When a bremsstrahlung photon is generated during a substep, the photon energy is subtracted from the projected electron energy at the end of the substep. Thus the radiative energy loss is explicitly taken into account, in contrast to the collisional (nonradiative) energy loss, which is treated probabilistically and is not correlated with the energetics of the substep. Two biasing techniques are available to modify the sampling of bremsstrahlung photons for subsequent transport. However, these biasing methods do not alter the linkage between the analog bremsstrahlung energy and the energetics of the substep.

MCNP uses identical physics for the transport of electrons and positrons, but distinguishes between them for tallying purposes, and for terminal processing. Electron and positron tracks are subject to the usual collection of terminal conditions, including escape (entering a region of zero importance), loss to time cutoff, loss to a variety of variance-reduction processes, and loss to energy cutoff. The case of energy cutoff requires special processing for positrons, which will annihilate at rest to produce two photons, each with energy mc^2 = 0.511008 MeV.

4. Collisional Stopping Power

Berger[4] gives the restricted electron collisional stopping power, *i.e.* the energy loss per unit path length to collisions resulting in fractional energy transfers ε less than an arbitrary maximum value ε_m, in the form

$$-\left(\frac{dE}{ds}\right)_{\varepsilon_m} = NZC\left\{\log\frac{E^2(\tau+2)}{2I^2} + \boldsymbol{f}^-(\tau, \varepsilon_m) - \delta\right\} \quad , \tag{3}$$

where

$$\boldsymbol{f}^-(\tau, \varepsilon_m) = -1-\beta^2+\left(\frac{\tau}{\tau+1}\right)^2\frac{\varepsilon_m^2}{2} + \frac{2\tau+1}{(\tau+1)^2}\log(1-\varepsilon_m) + \log[4\varepsilon_m(1-\varepsilon_m)] + \frac{1}{1-\varepsilon_m}. \tag{4}$$

Here ε and ε_m represent energy transfers as fractions of the electron kinetic energy E; I is the mean ionization potential in the same units as E; β is v/c; τ is the electron kinetic

energy in units of the electron rest mass; δ is the density effect correction (related to the polarization of the medium); Z is the average atomic number of the medium; N is the atom density of the medium in cm^{-3}; and the coefficient C is given by

$$C = \frac{2\pi e^4}{mv^2} \quad , \tag{5}$$

where m, e, and v are the rest mass, charge, and speed of the electron, respectively.

The ETRAN codes and MCNP do not make use of restricted stopping powers, but rather treat all collisional events in an uncorrelated, probabilistic way. Thus, only the total energy loss to collisions is needed, and Equations 3–4 can be evaluated for the special value $\varepsilon_m = 1/2$. The reason for the $1/2$ is the indistinguishability of the two outgoing electrons. The electron with the larger energy is, by definition, the primary. Therefore, only the range $\varepsilon \le 1/2$ is of interest. With $\varepsilon_m = 1/2$, Equation 4 becomes

$$f^-(\tau, \varepsilon_m) = -\beta^2 + 1 - \log 2 + \left(\frac{1}{8} + \log 2\right)\left(\frac{\tau}{\tau+1}\right)^2 \quad . \tag{6}$$

On the right side of Equation 3, we can express both E and I in units of the electron rest mass. Then E can be replaced by τ on the right side of the equation. We also introduce supplementary constants

$$C_2 = \log(2I^2) \quad ,$$

$$C_3 = 1 - \log 2 \quad ,$$

$$C_4 = \frac{1}{8} + \log 2 \quad , \tag{7}$$

so that Equation 3 becomes

$$-\left(\frac{dE}{ds}\right) = NZ\frac{2\pi e^4}{mv^2}\left\{\log[\tau^2(\tau+2)] - C_2 + C_3 - \beta^2 + C_4\left(\frac{\tau}{\tau+1}\right)^2 - \delta\right\} \quad . \tag{8}$$

This is the collisional energy loss rate in MeV/cm in a particular medium. In MCNP, we are actually interested in the energy loss rate in units of MeV $\cdot$ barns (so that different cells containing the same material need not have the same density). Therefore, we divide Equation 8 by N and multiply by the conversion factor 10^{24} barns/cm^2. We also use the definition of the fine structure constant

$$\alpha = \frac{2\pi e^2}{hc} ,$$

where h is Planck's constant, to eliminate the electronic charge e from Equation 8. The result is as follows:

$$-\left(\frac{dE}{ds}\right) = \frac{10^{24}\alpha^2 h^2 c^2 Z}{2\pi mc^2\beta^2}\left\{\log[\tau^2(\tau+2)] - C_2 + C_3 - \beta^2 + C_4\left(\frac{\tau}{\tau+1}\right)^2 - \delta\right\} . \qquad (9)$$

This is the form actually used in the code to preset the collisional stopping powers at the energy boundaries of the major energy steps.

5. Energy Straggling

Because an energy step represents the cumulative effect of many individual random collisions, fluctuations in the energy loss rate will occur. Thus the energy loss will not be a simple average $\bar{\Delta}$; rather there will be a probability distribution $f(s, \Delta)d\Delta$ from which the energy loss Δ for the step of length s can be sampled. Landau[2] studied this situation under the simplifying assumptions that the mean energy loss for a step is small compared with the electron's energy, that the energy parameter ξ defined below is large compared with the mean excitation energy of the medium, that the energy loss can be adequately computed from the Rutherford[7] cross section, and that the formal upper limit of energy loss can be extended to infinity. With these simplifications, Landau found that the energy loss distribution can be expressed as

$$f(s, \Delta)d\Delta = \phi(\lambda)d\lambda ,$$

in terms of $\phi(\lambda)$, a universal function of a single scaled variable

$$\lambda = \frac{\Delta}{\xi} - \log\left[\frac{2\xi mv^2}{(1-\beta^2)I^2}\right] + \delta + \beta^2 - 1 + \gamma . \qquad (10)$$

Here m and v are the mass and speed of the electron, δ is the density effect correction, β is v/c, I is the mean excitation energy of the medium, and γ is Euler's constant (γ = 0.5772157…). The parameter ξ is defined by

$$\xi = \frac{2\pi e^4 NZ}{mv^2} s ,$$

where e is the charge of the electron and NZ is the number density of atomic electrons. The universal function is

$$\phi(\lambda) = \frac{1}{2\pi i}\int_{x-i\infty}^{x+i\infty} e^{\mu\log\mu + \lambda\mu} d\mu ,$$

where x is a positive real number specifying the line of integration.

For purposes of sampling, $\phi(\lambda)$ is negligible for $\lambda < -4$, so that this range is ignored. Börsch-Supan[8] originally tabulated $\phi(\lambda)$ in the range $-4 \le \lambda \le 100$, and derived for the range $\lambda > 100$ the asymptotic form

$$\phi(\lambda) \approx \frac{1}{w^2 + \pi^2} \quad , \tag{11}$$

in terms of the auxiliary variable w, where

$$\lambda = w + \log w + \gamma - 3/2 \quad . \tag{12}$$

Recent extensions[9] of Börsch-Supan's tabulation have provided a representation of $\phi(\lambda)$ in the range $-4 \le \lambda \le 100$ in the form of five thousand equally probable bins in λ. In MCNP, the boundaries of these bins are saved in the array **eqlm(mlam)**, where the parameter **mlam** = 5001. Sampling from this tabular distribution accounts for approximately 98.96% of the cumulative probability for $\phi(\lambda)$. For the remaining large-λ tail of the distribution, MCNP uses the approximate form $\phi(\lambda) \approx w^{-2}$, which is easier to sample than Equation 11, but is still quite accurate for $\lambda > 100$.

Blunck and Leisegang[3] have extended Landau's result to include the second moment of the expansion of the cross section. Their result can be expressed as a convolution of Landau's distribution with a Gaussian distribution:

$$f^*(s, \Delta) = \frac{1}{\sqrt{2\pi}\sigma}\int_{-\infty}^{\infty} f(s, \Delta')\exp\left[-\frac{(\Delta - \Delta')^2}{2\sigma^2}\right] d\Delta' \quad .$$

Blunck and Westphal[10] provided a simple form for the variance of the Gaussian:

$$\sigma_{BW}^2 = 10\text{eV} \cdot Z^{4/3}\overline{\Delta} \quad .$$

Subsequently, Chechin and Ermilova[11] investigated the Landau/Blunck-Leisegang theory, and derived an estimate for the relative error

$$\varepsilon_{CE} \approx \left[\frac{10\xi}{I}\left(1 + \frac{\xi}{10I}\right)^3\right]^{-1/2}$$

due to the neglect of higher-order moments. Based on this work, Seltzer[12] describes and recommends a correction to the Blunck-Westphal variance:

$$\sigma = \frac{\sigma_{BW}}{1 + 3\varepsilon_{CE}} \quad .$$

This value for the variance of the Gaussian is used in MCNP.

Examination of Equations 10–12 shows that unrestricted sampling of λ will not result in a finite mean energy loss. Therefore, a material- and energy-dependent cutoff λ_c is imposed on the sampling of λ. In the initiation phase of an MCNP calculation, the code makes use of two preset arrays, **flam(mlanc)** and **avlm(mlanc)**, with **mlanc** = 1591. The array **flam** contains candidate values for λ_c in the range $-4 \le \lambda_c \le 50000$; the array **avlm** contains the corresponding expected mean values for the sampling of λ. For each material and electron energy, the code uses the known mean collisional energy loss $\bar{\Delta}$, interpolating in this tabular function to select a suitable value for λ_c, which is then stored in the dynamically-allocated array **flc**. During the transport phase of the calculation, the value of **flc** applicable to the current material and electron energy is used as an upper limit, and any sampled value of λ greater than the limit is rejected. In this way, the correct mean energy loss is preserved.

6. Angular Deflections

The ETRAN codes and MCNP rely on the Goudsmit-Saunderson[1] theory for the probability distribution of angular deflections. The angular deflection of the electron is sampled once per substep according to the distribution

$$F(s, \mu) = \sum_{j=0}^{\infty} \left(j + \frac{1}{2}\right) \exp(-sG_j) P_j(\mu) \quad ,$$

where s is the length of the substep, $\mu = \cos\theta$ is the angular deflection from the direction at the beginning of the substep, $P_j(\mu)$ is the jth Legendre polynomial, and G_j is

$$G_j = 2\pi N \int_{-1}^{1} \frac{d\sigma}{d\Omega} [1 - P_j(\mu)] d\mu \quad ,$$

in terms of the microscopic cross section $d\sigma/d\Omega$, and the atom density N of the medium.

For electrons with energies below 0.256 MeV, the microscopic cross section is taken from numerical tabulations developed from the work of Riley.[13] For higher-energy electrons, the microscopic cross section is approximated as a combination of the Mott[14] and Rutherford[7] cross sections, with a screening correction. Seltzer[5] presents this "factored cross section" in the form

$$\frac{d\sigma}{d\Omega} = \frac{Z^2e^2}{p^2v^2(1-\mu+2\eta)^2}\left[\frac{(d\sigma/d\Omega)_{\text{Mott}}}{(d\sigma/d\Omega)_{\text{Rutherford}}}\right] ,$$

where e, p, and v are the charge, momentum, and speed of the electron, respectively. The screening correction η was originally given by Molière[15] as

$$\eta = \frac{1}{4}\left(\frac{\alpha mc}{0.885p}\right)^2 Z^{2/3}\left[1.13 + 3.76\left(\frac{\alpha Z}{\beta}\right)^2\right] ,$$

where α is the fine structure constant, m is the rest mass of the electron, and $\beta = v/c$. MCNP now follows the recommendation of Seltzer,[5] and the implementation in the Integrated TIGER Series, by using the slightly modified form

$$\eta = \frac{1}{4}\left(\frac{\alpha mc}{0.885p}\right)^2 Z^{2/3}\left[1.13 + 3.76\left(\frac{\alpha Z}{\beta}\right)^2 \sqrt{\frac{\tau}{\tau+1}}\right] ,$$

where τ is the electron energy in units of electron rest mass. The multiplicative factor in the final term is an empirical correction which improves the agreement at low energies between the factored cross section and the more accurate partial-wave cross sections of Riley.

Before the transport phase, MCNP calculates energy-dependent values of $F(s, \mu)$ for the predetermined substep lengths s in each material. The results are stored as a histogram giving the probabilities for 33 standard angular bins used to sample the angular deflection. Because of the highly forward-peaked nature of the electron scattering, a better approximation of the angular distribution is obtained if a separate delta function component representing zero angular deflection is included. Therefore, MCNP also accounts for the probability of zero scattering before electing to sample from the angular distribution. This aspect of the angular distribution becomes more important when the number of substeps per energy step in increased, or when many partial substeps must be taken. The latter case occurs when the electron substep is frequently interrupted by geometric boundaries, by the problem time cutoff, or by the sampling of secondary particles.

When an electron makes only a partial substep, it is also necessary to approximate the Goudsmit-Saunderson distribution for a pathlength shorter than the preselected substep length. MCNP handles this situation by first considering the zero-deflection probability, and then interpolating the angular distribution. Specifically, if $P_Z(1)$ is the probability of zero deflection for a full substep, and if f is the fraction of a substep to be taken, then the power law $P_Z(f) = [P_Z(1)]^f$ gives the probability of zero deflection for the partial substep. When zero deflection is not selected, then the full-substep Goudsmit-Saunderson distribution is sampled for a deflection cosine μ. Then the actual deflection for the partial substep is obtained by linear interpolation in the cosine: $\cos\mu' = 1 - f(1 - \cos\mu)$.

7. Bremsstrahlung

For the sampling of bremsstrahlung photons, MCNP relies primarily on the Bethe-Heitler[16] Born-approximation results that have been used until rather recently[17] in ETRAN. A comprehensive review of bremsstrahlung formulas and approximations relevant to the present level of the theory in MCNP can be found in the paper of Koch and Motz.[18] Particular prescriptions appropriate to Monte Carlo calculations have been developed by Berger and Seltzer.[19] For the ETRAN-based codes, this body of data has been converted to tables including bremsstrahlung production probabilities, photon energy distributions, and photon angular distributions.

MCNP addresses the sampling of bremsstrahlung photons at each electron substep. The tables of production probabilities are used to determine whether a bremsstrahlung photon will be created. If so, the new photon energy is sampled from the energy distribution tables. By default, the angular deflection of the photon from the direction of the electron is also sampled from the tabular data. The direction of the electron is unaffected by the generation of the photon, because the angular deflection of the electron is controlled by the multiple scattering theory. However, the energy of the electron at the end of the substep is reduced by the energy of the sampled photon, because the treatment of electron energy loss, with or without straggling, is based only on nonradiative processes.

There is an alternative to the use of tabular data for the angular distribution of bremsstrahlung photons. If the fourth entry on the PHYS:E card is 1, then the simple, material-independent probability distribution

$$f(\mu)d\mu = \frac{1-\beta^2}{2(1-\beta\mu)^2}d\mu \ , \tag{13}$$

where $\mu = \cos\theta$ and $\beta = v/c$, will be used to sample for the angle of the photon relative to the direction of the electron. This sampling method is of interest only in the context of detectors and DXTRAN spheres. A set of source contribution probabilities $p(\mu)$ reflecting the tabular data is not available. Therefore, detector and DXTRAN source contributions are made using Equation 13. An option exists to specify that the generation of bremsstrahlung photons rely on Equation 13 as well, thus forcing the actual transport to be consistent with the source contributions to detectors and DXTRAN. However, this option is primarily of interest only to code developers.

8. Knock-On Electrons

The Møller cross section[20] for the scattering of an electron by an electron is

$$\frac{d\sigma}{d\varepsilon} = \frac{C}{E}\left\{\frac{1}{\varepsilon^2} + \frac{1}{(1-\varepsilon)^2} + \left(\frac{\tau}{\tau+1}\right)^2 - \frac{2\tau+1}{(\tau+1)^2}\frac{1}{\varepsilon(1-\varepsilon)}\right\} \ , \tag{14}$$

where ε, τ, E, and C have the same meanings as in Equations 3–5. When calculating stopping powers, one is interested in all possible energy transfers. However, for the sampling of transportable secondary particles, one wants the probability of energy transfers greater than some ε_c representing an energy cutoff, below which secondary particles will not be followed. This probability can be written

$$\sigma(\varepsilon_c) = \int_{\varepsilon_c}^{1/2} \frac{d\sigma}{d\varepsilon} d\varepsilon \ .$$

The reason for the upper limit of 1/2 is the same as in the discussion of Equation 6. Explicit integration of Equation 14 leads to

$$\sigma(\varepsilon_c) = \frac{C}{E}\left\{\frac{1}{\varepsilon_c} - \frac{1}{1-\varepsilon_c} + \left(\frac{\tau}{\tau+1}\right)^2\left(\frac{1}{2} - \varepsilon_c\right) - \frac{2\tau+1}{(\tau+1)^2}\log\frac{1-\varepsilon_c}{\varepsilon_c}\right\} \ .$$

Then the normalized probability distribution for the generation of secondary electrons with $\varepsilon > \varepsilon_c$ is given by

$$g(\varepsilon, \varepsilon_c)d\varepsilon = \frac{1}{\sigma(\varepsilon_c)}\frac{d\sigma}{d\varepsilon}d\varepsilon \ . \tag{15}$$

At each electron substep, MCNP uses $\sigma(\varepsilon_c)$ to determine randomly whether knock-on electrons will be generated. If so, the distribution of Equation 15 is used to sample the energy of each secondary electron. Once an energy has been sampled, the angle between the primary direction and the direction of the newly generated secondary particle is determined by momentum conservation. This angular deflection is used for the subsequent transport of the secondary electron. However, neither the energy nor the direction of the primary electron is altered by the sampling of the secondary particle. On the average, both the energy loss and the angular deflection of the primary electron have been taken into account by the multiple scattering theories.

References

1. S. Goudsmit and J. L. Saunderson, "Multiple Scattering of Electrons," *Phys. Rev.* **57** (1940) 24.

2. L. Landau, "On the Energy Loss of Fast Particles by Ionization," *J. Phys. USSR* **8** (1944) 201.

3. O. Blunck and S. Leisegang, "Zum Energieverlust schneller Elektronen in dünnen Schichten," *Z. Physik* **128** (1950) 500.

4. M. J. Berger, “Monte Carlo Calculation of the Penetration and Diffusion of Fast Charged Particles,” in *Methods in Computational Physics*, Vol. 1, edited by B. Alder, S. Fernbach, and M. Rotenberg, (Academic Press, New York, 1963) 135.

5. Stephen M. Seltzer, “An Overview of ETRAN Monte Carlo Methods,” in *Monte Carlo Transport of Electrons and Photons*, edited by Theodore M. Jenkins, Walter R. Nelson, and Alessandro Rindi, (Plenum Press, New York, 1988) 153.

6. J. Halbleib, “Structure and Operation of the ITS Code System,” in *Monte Carlo Transport of Electrons and Photons*, edited by Theodore M. Jenkins, Walter R. Nelson, and Alessandro Rindi, (Plenum Press, New York, 1988) 249.

7. E. Rutherford, “The Scattering of α and β Particles by Matter and the Structure of the Atom,” *Philos. Mag.* **21** (1911) 669.

8. W. Börsch-Supan, “On the Evaluation of the Function

$$\phi(\lambda) = \frac{1}{2\pi i}\int_{x-i\infty}^{x+i\infty} e^{\mu\log\mu + \lambda\mu} d\mu$$

for Real Values of λ,” *J. Res. National Bureau of Standards* **65B** (1961) 245.

9. J. A. Halbleib, R. P. Kensek, T. A. Mehlhorn, G. D. Valdez, S. M. Seltzer, and M. J. Berger, “ITS Version 3.0: The Integrated TIGER Series of Coupled Electron/Photon Monte Carlo Transport Codes,” Sandia National Laboratories report SAND91–1634 (March 1992).

10. O. Blunck and K. Westphal, “Zum Energieverlust energiereicher Elektronen in dünnen Schichten,” *Z. Physik* **130** (1951) 641.

11. V. A. Chechin and V. C. Ermilova, “The Ionization-Loss Distribution at Very Small Absorber Thickness,” *Nucl. Instr. Meth.* **136** (1976) 551.

12. Stephen M. Seltzer, “Electron-Photon Monte Carlo Calculations: The ETRAN Code,” *Appl. Radiat. Isot.* Vol. 42, No. 10 (1991) pp. 917–941.

13. M. E. Riley, C. J. MacCallum, and F. Biggs, “Theoretical Electron-Atom Elastic Scattering Cross Sections. Selected Elements, 1 keV to 256 keV,” *Atom. Data and Nucl. Data Tables* **15** (1975) 443.

14. N. F. Mott, “The Scattering of Fast Electrons by Atomic Nuclei,” *Proc. Roy. Soc. (London)* **A124** (1929) 425.

15. G. Molière, “Theorie der Streuung schneller geladener Teilchen II: Mehrfach- und Vielfachstreuung,” *Z. Naturforsch.* **3a** (1948) 78.

16. H. A. Bethe and W. Heitler, “On Stopping of Fast Particles and on the Creation of Positive Electrons,” *Proc. Roy. Soc. (London)* **A146** (1934) 83.

17. Stephen M. Seltzer, "Cross Sections for Bremsstrahlung Production and Electron Impact Ionization," in *Monte Carlo Transport of Electrons and Photons*, edited by Theodore M. Jenkins, Walter R. Nelson, and Alessandro Rindi, (Plenum Press, New York, 1988) 81.

18. H. W. Koch and J. W. Motz, "Bremsstrahlung Cross-Section Formulas and Related Data," *Rev. Mod. Phys.* **31** (1959) 920.

19. Martin J. Berger and Stephen M. Seltzer, "Bremsstrahlung and Photoneutrons from Thick Tungsten and Tantalum Targets," *Phys. Rev.* **C2** (1970) 621.

20. C. M∅ller, "Zur Theorie des Durchgang schneller Elektronen durch Materie," *Ann. Physik.* **14** (1932) 568.